CAPABILITY OF NOL BALLISTICS RANGES FOR OBTAINING

SPHERE DRAG COEFFICIENT DATA

By W. Carson Lyons, Jr.

U. S. Naval Ordnance Laboratory, White Oak

SUMMARY

Descriptions of three ballistics range facilities at the Naval Ordnance Laboratory are presented. The Mach number-Reynolds number capability for each facility is shown for the case of obtaining drag coefficients of spheres. It is shown that these three facilities can cover most of the Mach number-Reynolds number field between Mach numbers of 0.1 and 22 and between Reynolds numbers of 10^1 and 10^7. A discussion of various sources of errors involved in measuring sphere drag coefficients in a ballistics range and of estimates of the magnitude of the errors is presented.

INTRODUCTION

The well-equipped, modern, ballistics range represents a unique facility for determining the aerodynamic drag and stability characteristics of projectiles in free flight. These projectiles can be intricate models of full-scale vehicles, full-scale armament projectiles, or a very simple aerodynamic shape, such as a sphere. Part of the uniqueness of this type of facility is the wide range of test conditions that can be achieved for the simulation of various flight environments. Of the various measurements that can be made in a ballistics range, the drag coefficient is determined with the highest degree of accuracy.

Although there are many ballistics ranges in operation in the United States, the three aerodynamic-aerophysics ranges at the Naval Ordnance Laboratory form a good representation of ballistics range capabilities. Therefore, no attempt will be made to present a survey of ballistics ranges and their capabilities in general. Most of the discussion of measurements of drag coefficients will apply to any model configuration, although, where it is necessary to be more specific, only the determination of the drag of spheres will be considered.

SYMBOLS

a   speed of sound or semimajor axis of an ellipse

A   reference area

b   semiminor axis of an ellipse

c   constant in linear drag coefficient relation; Eq. (8)

C_D drag coefficient

C_{p_M} maximum pressure coefficient

f   constant in linear drag coefficient relation; Eq. (8)

g   acceleration of gravity

m   mass of projectile

M   Mach number

Re   Reynolds number

Re_d Reynolds number based on sphere diameter

t   time

V   velocity

W   weight of projectile

Y   vertical distance in the ballistics range measured from range centerline

Z   longitudinal distance in the ballistics range

β ballistic parameter $(W/C_D A)$

ρ gas density

σ standard deviation

Subscripts:

m   indicates midrange conditions

o   indicates initial conditions

∞ indicates free-stream conditions

DESCRIPTION OF FACILITIES

There are three ballistics ranges currently being operated at the Naval Ordnance Laboratory suitable for making either drag or drag and stability measurements. They vary from a small, 5-inch-diameter, 300-foot-long facility referred to as the Aerophysics Range to the largest of NOL's range facilities, which is 10 feet in diameter and 1000 feet long, referred to as the 1000-foot Hyperballistics Range. The third facility, an intermediate size facility, is called the Pressurized Ballistics Range. A description of each of these three facilities, their instrumentation, and their testing capabilities will be presented.

1000-Foot Hyperballistics Range (HBR)

This facility consists of a 10-foot-diameter, 1000-foot-long steel tube. Models are launched into this testing chamber using a two-stage, light gas gun. An artist's drawing of the launcher and a portion of the steel tube and supporting structure is shown in figure 1. The ambient pressure of the air within the 1000-foot-long test chamber can be varied from one atmosphere down to approximately 0.5 torr. The temperature of the air in the tube is maintained at approximately 65°F. Although most tests are conducted in air, a nitrogen atmosphere can be substituted for tests that require pressures of only 200 torr or less.

Instrumentation for conducting drag and stability tests currently includes 37 dual-plane spark shadowgraph stations covering a testing length of 870 feet. Figure 2 is a photograph of the inside of the 10-foot-diameter tube showing some of these stations. Each station consists of two barium-titanate spark light sources, two cameras, two 4-foot-diameter spherical reflectors, and a model detection system. A schematic drawing of one of these stations is shown in figure 3. It is seen from this drawing that, although the range tube is 10 feet in diameter, the usable cross section is approximately a 22-inch-diameter circle in the center of the tube. The model detection system with which each of the 37 shadowgraph stations is equipped detects the model and activates the spark light source when the model is in the field of view of the station. This system has sufficient sensitivity to detect spheres as small as 3/16 inch flying in this facility.

The model launcher used with this facility is a two-stage, light gas gun currently having a 2-inch, smooth-bore launch tube, 80 feet long. A 4-inch-inside-diameter launch tube is also available for this gun. Hydrogen is used as the working gas to launch the models. Slender conical models have been launched at velocities in excess of 25,000 ft/sec. Spheres can be launched at even higher velocities.

The first 80 feet of the 1000-foot test chamber are separated from the remainder of the range by a bulkhead having a 13-inch-diameter hole on the range centerline. This 13-inch hole is further restricted to 3 inches for most tests. This section of the range is referred to as the blast tank and is used to catch the hydrogen following the model out of the gun barrel. The sabot used in launching the model is stripped from the model and impacts in this section. Three short-duration X-ray stations are mounted in this section to monitor the separation of the sabot from the model and to determine the structural integrity of the model after undergoing the high-acceleration phase of launching. The stations are located 6.5, 16.5 and 26.5 feet from the gun muzzle.

Pressurized Ballistics Range (PBR)

The Pressurized Ballistics Range utilizes a steel tube, 300 feet long and 3 feet in diameter, as a test chamber. A variety of guns can be mounted at one end of this tube for launching models. The pressure of the test gas within this facility can be adjusted from five atmospheres to approximately two torr. Except for a 20-foot-long special instrumentation section, the temperature of the gas in this range is maintained at 74°F. In the 20-foot-long special instrumentation section, the temperature can be varied from -280° to +1000°F. Tests in gases other than air can readily be conducted in this facility (ref. 1). A gas chromatograph and a mass spectrometer are available for monitoring the constituents of the test gas at five locations along the tube.

Twenty-seven dual-plane shadowgraph stations are used to determine the trajectory of a model flying in the range. The stations cover a usable testing length of 188 feet. These stations are directly illuminated shadowgraphs. A short-duration spark light source on one side of the range tube directly illuminates a vertical, 14x17-inch glass photographic plate. Light from this single light source is reflected off a flat-faced mirror at the top of the tube to illuminate a horizontal photographic plate located at the bottom of the tube. This results in a set of pictures of the model in orthogonal planes at each of the 27 stations. A sketch of one of these stations is shown in figure 4. Each station is equipped with a model detection and triggering system.

For velocities up to approximately 5000 ft/sec, several different size powder-driven guns are available for model launching. Velocities greater than 5000 ft/sec require the use of a two-stage, light gas gun. This gun can launch models at velocities up to approximately 22,000 ft/sec and has a 1.3-inch-inside-diameter launch tube.

This facility is equipped with a blast tank in which the sabot is stripped from the model and in which most of the driving gases are retained. Two X-ray stations in the blast tank monitor the separation of the sabot from the model shortly after they emerge from the gun muzzle.

Aerophysics Range (APR)

The Aerophysics Range consists of a 5-inch-diameter test chamber, 350 feet long. Models are launched down this tube using a two-stage, light gas gun. The pressure of the test gas in this facility can be controlled from one atmosphere down to 0.2 torr. The test gas is also maintained at room temperature. A photograph of this facility is shown in figure 5. Because of the small volume of this test chamber, various test gases can conveniently be used.

The instrumentation in this facility for measuring drag coefficients consists of four single-plane, high-resolution, rotating-mirror camera stations and associated detection and triggering units.

Velocities up to 23,000 ft/sec are achieved with a two-stage, light gas gun having a smooth-bore barrel 0.375 inch in diameter.

The initial 18 feet of the range tube form the blast tank for this facility. As described for the other two facilities, the sabot is removed from the model and captured in this chamber.

TEST CONDITIONS

The drag coefficient of a sphere has been discussed thoroughly by many authors and investigators (for example, refs. 2, 3, and 4). The purpose of this current discussion will be to reiterate the pertinent similarity parameters for different flow regimes that must be duplicated when performing scaled experiments in ground-based test facilities.

Flow regimes can be specified as indicated by Tsien (ref. 5) by ratios of the Mach number to Reynolds number functions. These flow regimes are illustrated in figure 6. The continuum flow regime is represented by the two regions defined by $M/\sqrt{Re} \leq 0.1$. The ordinary gas dynamic regime is a continuum flow regime where it is assumed that "no slip" (zero fluid velocity) occurs at a body surface, while, in the slip flow regime, the flow is considered continuum but a finite velocity is assumed to exist at a body surface. For values of $M/Re \geq 10$ (this is representative

of large Knudsen numbers), the flow is considered in the free
molecular regime. Between the slip flow continuum regime
and the free molecular regime, there is a transitional region.

Within these flow regimes sphere velocities can be subsonic,
supersonic, or in the transonic region. It can be shown, in
general, that to duplicate the drag coefficient of a sphere, it
is sufficient to duplicate the Mach number and the Reynolds
number. In rarefied gas flow regimes, the Knudsen number is a
significant parameter. However, the Knudsen number can be
expressed approximately as a Mach number-Reynolds number function.

Figure 7 is a plot of the drag coefficient for a sphere as
a function of Mach number, for continuum flow. The two branches
of the curve in the subsonic region reflect the difference in
the drag coefficient for a subcritical and a supercritical
Reynolds number. The curves in figure 7 were compiled from
information in reference 2.

One current use of accurate measurements of drag coeffi-
cients of spheres is in the determination of the atmospheric
density at various altitudes from descending sphere experiments.
In these experiments spheres are launched to high altitudes,
released, and allowed to fall. The trajectory of the sphere is
then determined, usually by radar tracking. Since the trajectory
of the sphere is uniquely a function of the atmospheric density
and the ballistic parameter $(W/C_D A)$ of the sphere, accurate
measurements of the drag coefficient, weight, and size of the
sphere, along with the trajectory information, allow the density
to be determined. To illustrate Mach numbers and corresponding
Reynolds numbers for a typical free-fall balloon trajectory,
calculations have been performed for three different size-
weight combination balloons. For all three cases trajectories
were calculated by assuming that the spheres started falling
with zero velocity from an altitude of 300,000 feet. During
actual tests two of the balloon systems are carried to their
release altitude using a Nike-Cajun sounding rocket. The one-
meter balloon is part of the Robin system. The Mach number-
Reynolds number trajectory resulting from these calculations is
presented in figure 8. Although the maximum Mach number attained
during the flight of any of these three example spheres does not
exceed 3, nor the Reynolds number exceed 1×10^6, tests in a
ballistics range can be conducted at much higher Mach numbers
and slightly higher Reynolds numbers.

From the discussion on drag coefficients it was shown that,
except for a few certain flow regimes, both the Mach number and
the Reynolds number must be duplicated when performing scaled-
model tests to determine the drag coefficient for spheres. It
is, therefore, appropriate to show the Mach number-Reynolds
number field which can be covered by the three ballistics range

facilities described earlier. The Mach number that can be attained in a ballistics range is only a function of the flight velocity of the projectile. The temperature of the test gas, and hence the speed of sound in the test gas, is essentially a fixed value. For air at room temperature, the speed of sound is approximately 1140 ft/sec. Hence, $M\infty = V\infty/1140$, where $V\infty$ is expressed in feet per second. The pressure of the air in a ballistics range can be set at any desired value, commensurate with the pumping capability and structural strength of the test chamber, and is independent from the flight Mach number. Since the temperature is essentially a fixed value, the Reynolds number can be expressed for room temperature air as

$$Re_d = 0.57 \ P_\infty M_\infty \ d \ x \ 10^6 \tag{1}$$

where P_∞ is expressed in atmospheres and the sphere diameter, d, in inches. The maximum-diameter sphere that can be launched at various Mach numbers in the Hyperballistics Range and the Pressurized Ballistics Range is shown in figure 9. These sphere diameters were used in computing the maximum Reynolds numbers that can be achieved.

The maximum and minimum Mach number-Reynolds number envelope for the supersonic and hypersonic regime that can be achieved in the three ballistics range facilities is shown in figure 10. Only the boundary of the envelope unique to each particular facility is shown. A large region of overlap among all three facilities exists in the center portion of the envelope. This envelope is based on the use of the two-stage, light gas guns available for use in each of the three facilities.

The upper boundary of the envelope is dictated by the maximum velocity that can be achieved reliably with the gas gun model launchers. The Hyperballistics Range can achieve a Mach number of 22, while the other two ranges can achieve a Mach number of 20.

The maximum Reynolds numbers for Mach numbers of 20 or less (see the right-hand boundary of the envelope) are achieved in the Pressurized Ballistics Range. Even though larger spheres can be launched in the Hyperballistics Range, larger Reynolds numbers can be obtained in the Pressurized Ballistics Range, since it can be operated at a pressure of five atmospheres, five times greater than the HBR. The smallest Reynolds numbers for Mach numbers between approximately 2 and 20 are obtained in the Aerophysics Range. These Reynolds numbers are based on sphere diameters of 400 microns and range pressures of 0.2 torr. Tests using spheres this small can only be conducted in this facility, since it is the only facility that has a model detection and triggering system for the instrumentation sensitive enough to detect a sphere only 400 microns in diameter.

The minimum Mach number forming the lower boundary of the envelope, shown in figure 10, is a result of the usable cross section of each of the three facilities involved. The usable cross section for the HBR is approximately a 22-inch circle in the center of the 10-foot-diameter tube formed by the field of view of the instrumentation. This can be seen in figure 3. Steel baffle plates having a 13-inch square opening in the center separate each instrument station in the PBR. These openings restrict the usable cross section in this facility. The 5-inch diameter of the Aerophysics Range tube represents the usable cross section of this facility. For supersonic and hypersonic testing, the gas guns are used. The centerlines of the launch tube of these guns are aligned to coincide with the centerline of the range tube. If the launch velocity of a projectile is too low, the projectile will drop out of the usable cross section of the range before traveling a sufficient length downrange to allow a drag coefficient measurement to be made. The minimum Mach number has been calculated from the relation

$$
M_{min} = \frac{2\beta}{a_\infty \rho_\infty} \sqrt{\frac{g}{2Y}} \left(e^{\frac{\rho_\infty Z}{2\beta}} - 1 \right) \tag{2}
$$

In this relation Y is the allowable vertical drop. This is 11 inches, 6.5 inches, and 2.5 inches for the HBR, PBR, and APR, respectively. The value of Z used was 300 feet, 236 feet, and 300 feet for the HBR, PBR, and APR, respectively. Minimum Mach numbers were calculated only for the maximum and minimum Reynolds numbers for each of the three facilities. Straight lines were then used to connect these points to form the lower boundary of the envelope in figure 10.

For low supersonic and subsonic testing, only the Pressurized Ballistics Range can be used presently. In addition to the gas gun, smaller powder-driven guns are available for use in this facility. The centerline of the barrel of these powder-driven guns can be elevated at various angles with respect to the centerline of the range tube. This allows, with the gun set at the proper elevation angle, the full 13-inch usable cross section of the PBR to be used, rather than just half of it as is the case with the gas gun. Further, the location of the powder gun when mounted in the PBR puts the muzzle 13 feet from the first usable shadowgraph station. The first usable station in this case is station number 4, which limits the total number of instrumentation stations to 24. Using standard projectile ballistic equations (see, for instance, ref. 6), trajectories of a 2-inch-diameter sphere have been calculated for initial Mach numbers from 0.1 to 0.6 and a range pressure of 5 atmospheres. These calculations were performed for the gun aligned at an

elevation angle that allows almost complete use of the usable
13-inch-square cross section of the PBR. These trajectories
have been plotted in figure 11. For M_∞ = 0.1, a flight of approx-
imately 36 feet of instrumented length can be achieved. This
will allow the sphere to be observed at five stations. For
M_∞ = 0.2, the sphere can be observed by 12 stations. For initial
Mach numbers of 0.6 or greater, a 2-inch sphere flying in air at
a pressure of 5 atmospheres will travel the full length of the
range. The calculations represent the highest Reynolds numbers
that can be achieved at these subsonic Mach numbers. To investi-
gate the lowest Reynolds numbers that can be achieved at these
subsonic Mach numbers, additional calculations were performed
for a sphere having a 3/16-inch diameter and a range pressure of
2 torr. These calculations indicated slightly more favorable
conditions. A small increase in testing length was realized.

A Mach number-Reynolds number field for Mach numbers less
than 2 that can be achieved in the Pressurized Ballistics Range
is shown in figure 12. It can be seen by comparing figures 8,
10, and 12 that the Mach number and Reynolds number can both be
duplicated in one of the three ballistics range facilities for
a significant portion of a typical trajectory for a falling
balloon. Specifically, data at Mach numbers below approximately
0.1 cannot be obtained at any Reynolds number.

Further, data cannot be obtained at any Mach number for
Reynolds numbers less than approximately 3×10^1. Data can
be obtained for all other Mach number and Reynolds number com-
binations up to Mach number 20 and Reynolds numbers of 1×10^7.

DATA REDUCTION AND ESTIMATES OF ERRORS

The method used to obtain values for the drag coefficient
from ballistics range tests consists of fitting measured time-
distance points to an algebraic relation. This relation is
obtained from the longitudinal equation of motion for a projec-
tile flying in the ballistics range given as

$$-C_D\left(\frac{1}{2}\rho_\infty V^2\right)A = m\frac{dV_\infty}{dt} \tag{3}$$

Assuming a constant drag coefficient, this equation can be
solved to give

$$Z-Z_m = Z_0 + \frac{2\beta}{\rho_\infty}\ln\left[1 + \frac{\rho_\infty}{2\beta}V_\infty(t-t_m)\right] \tag{4}$$

where
$$\beta = W/C_D A$$

77

and Z_m and t_m are the values of the distance and time for the station nearest midrange. This equation is approximated by using the first three terms of the series expansion for the logarithmic function, and the resulting equation

$$Z-Z_m = Z_o+V_\infty\left(t-t_m\right) - \frac{\rho_\infty}{2\beta}\frac{V_\infty^2}{2}\left(t-t_m\right)^2+\left(\frac{\rho_\infty}{2\beta}\right)^2\frac{V_\infty^3}{3}\left(t-t_m\right)^3 \qquad (5)$$

is fitted by the method of least mean squares to the time-distance data. The drag coefficient and the velocity at the station nearest midrange are computed from the constants of Eq. (5). This, of course, requires that the mass of the model and the density of the test gas be measured prior to launching the model.

Using the shadowgraph stations in the ballistics ranges, the position of models can be determined to within ±0.002 foot and time to 2 x 10^{-7} seconds. The weight of a model, up to 1000 grams, is determined prior to launching, using NBS class S weights, and is considered to be accurate to within ±0.1 milligram. The diameter of a sphere is measured prior to launching to an accuracy of ±0.0001 inch.

The error in measuring the range pressure is less than 0.2 percent at pressure as low as 0.2 torr. The percent error is, of course, less as the range pressure being measured increases. The maximum leak rate at the lowest pressure in any of the ballistics ranges is 0.08 torr per minute. Normally the pumps are turned off approximately 30 seconds prior to launching the model. For tests conducted at very low pressures, where the leak rate might be significant, pumping can be maintained throughout launching.

The temperature of the test gas in the ballistics ranges is measured at three locations. As previously mentioned, the temperature is approximately 74°F and is measured to within ±0.1°F.

Some analyses have been performed to illustrate the magnitude of the error in C_D due to various effects. One effect considered is sphere distortion, where the body for which it is assumed a drag coefficient is being measured has been distorted into a nonspherical shape. Another effect considered is the use of a constant C_D data reduction method for reducing data from variable C_D trajectories. Finally, the effect of inaccuracies in distance measurements and number of available data stations will be discussed.

78

For high-velocity testing ($M_\infty > 15$) the spheres undergo very high accelerations during the launching phase of the test. It is conceivable that, under this high-inertial loading, a sphere of certain materials which do not possess sufficiently high strength might become distorted. Estimates have been made to determine the error induced in the drag coefficient resulting from distortion of the sphere. During launching it is assumed that it could become flattened. To represent the resulting body of revolution, an ellipse has been rotated about one of its axes to form an axisymmetric body. Using modified Newtonian impact theory, the drag coefficient of such a body is given as

$$C_{D_B} = \frac{C_{p_M}(b/a)^2}{(b/a)^2-1}\left[1 - \frac{1}{(b/a)^2-1}\ln(b/a)^2\right] \qquad (6)$$

The percent error induced by flattening a sphere is defined as

$$\%\Delta C_D = \frac{C_{D_B} - C_{D_S}}{C_{D_S}} \times 100 \qquad (7)$$

where C_{D_S} is the drag coefficient of a sphere given by Newtonian impact theory as $C_{D_S} = C_{p_M}/2$. The results of these calculations are shown in figure 13. It is seen from figure 13 that the curve is nearly linear. The error in drag coefficient for 1 percent flattening is approximately 0.6 percent. The curve has been plotted for two cases: The upper portion of the curve is for the case of the minor axis of the ellipse aligned with the velocity vector, while the lower portion of the curve is for the major axis aligned with the velocity vector.

As was illustrated in the section on drag coefficients, there is a large change in C_D with variation in Mach number in the transonic region ($0.6 \le M \le 1.75$). In the relations used for reducing the time-distance data to drag coefficients, it was assumed that the drag coefficient remained constant during a flight in the range. This assumption is certainly valid in the subsonic and hypersonic continuum flow region. However, in the transonic region this assumption is not valid, and significant changes in the drag coefficient can occur if the velocity decrement during a flight is too large. In practice, the drag coefficient derived from a test in the ballistics range is associated with the midrange Mach number, since there is always some change in velocity during a flight. To investigate the error in the drag coefficient resulting from a ballistics range test, Eq. (3) was solved for the case of C_D, varying linearly with velocity

(or Mach number for a constant range temperature), and expressed as

$$C_D = c + fV \qquad (8)$$

The solution of Eq. (3) is

$$Z = - \frac{2m}{\rho_\infty c A} \ln\frac{V}{V_O} \left(\frac{f + c/V_O}{f \ V/V_O + c/V_O} \right) \qquad (9)$$

The solution of Eq. (3) for the case of a constant drag coefficient $(c = C_D; \ f = 0)$ is

$$Z = - \frac{2\beta}{\rho_\infty} \ln \frac{V}{V_O} \qquad (10)$$

Equating Eqs. (9) and (10) and solving for C_D results in a relation for an average value of C_D computed from a variable C_D trajectory. This equation is given as

$$C_{D_A} = \frac{c \ \ln \frac{V}{V_O}}{\ln \frac{V}{V_O} \left(\frac{f + c/V_O}{f \ V/V_O + c/V_O} \right)} \qquad (11)$$

Notice that the average C_D is only a function of the initial velocity and the final-to-initial velocity ratio. As is the practice in ballistics-range data reduction, this C_D is associated with the Mach number which occurs at the midrange value of Z. Referring to Eq. (8), an exact value of C_D is

$$C_{D_E} = c + fV_m \qquad (12)$$

A percent error in C_D due to using a constant C_D data reduction method to reduce data obtained from a variable C_D trajectory can be defined as

$$\%\Delta C_D = \frac{C_{D_E} - C_{D_A}}{C_{D_E}} \times 100 \qquad (13)$$

80

Values of $\%\Delta C_D$ will be a function only of the initial velocity
and the final-to-initial velocity ratio, which can be expressed
as a percent velocity decrement. Calculations were performed
for initial velocities from 794 to 1475 ft/sec and for percent
velocity decrements from 0 to 38 percent. It was found that the
value of the initial velocity has a negligible effect on the
results. The percent error in C_D is shown as a function of the

percent velocity decrement in figure 14. It is seen that a
10 percent velocity decrement results in only 0.1 percent error
in C_D. Although it is recognized that this is an idealized

calculation, it does serve as a guide when performing tests in
a ballistics range in the transonic flow regime where there are
large variations in C_D with Mach number. The results also indi-
cate that, except for extremely large velocity changes, a negli-
gibly small error is incurred in the C_D measurement.

A digital computer program was utilized to illustrate the
effect of measuring accuracy, number of stations, and station
spacing in the NOL ranges on the accuracy of measured drag
coefficients. An "exact" time-distance trajectory was calculated
using the standard ballistic trajectory equations for a projectile
previously mentioned. It was then assumed that the times were
exact, but some error was incurred at each measuring station,
which alters the value of Z. It was assumed that the maximum
error or alteration in Z is ±0.002 foot. At each value of Z to
be perturbed, the computer chose at random an integral number
between 1 and 10. If this number was even, the perturbation in
Z was positive, while if the number was odd, the perturbation
was negative. The magnitude of the perturbation was determined
as follows: A Gaussian distribution curve was used in which
the peak of the curve is taken as zero along the ordinate to a
value of 1 at the origin of the ordinate. Along the abscissa
the peak of the curve corresponds to zero while the 3σ point
corresponds to 1. Again using the computer, a random number was
selected between 0 and 1. This number was located along the
abscissa which then specified a number between 0 and 1 along the
ordinate corresponding to the Gaussian curve being used. This
number obtained along the ordinate was multiplied by the maximum
possible error of 0.002 foot. The result was the magnitude of
the perturbation applied to the value of Z being considered.
Eq. (5) was then fitted to these new values of Z and their cor-
responding values of time. This allowed a value of C_D to be

determined for measurements considered obtained from a prescribed
number of stations, with a given distribution, and with a normal
distribution of error. For any set of conditions, this process
was performed ten times. The resulting drag coefficient from
each of the ten runs was compared to the original or "exact"
value of C_D used in performing the trajectory calculations. A

standard deviation is defined as

$$\sigma = \sqrt{\dfrac{\sum\limits_{i=0}^{10}\left[C_D(exact) - C_D(calculated)_i\right]^2}{10}}$$ (14)

A percent error in the drag coefficient is given by

$$\%\Delta C_D = \dfrac{2\sigma}{C_D(calculated)}$$ (15)

Using 2σ in determining the percent error means that 95 percent of the tests conducted will have percent errors equal to or less than the value given by Eq. (15). Using this analysis, selected Mach number-Reynolds number conditions were investigated. Since the error incurred for any particular condition is a function of the deceleration of the projectile, for each Mach number-Reynolds number condition several different combinations of sphere diameter and range pressures were used. Calculations were made for both copper and lexan spheres, giving a large difference in the material density and, hence, their trajectory. This allowed a selection of the near minimum error to be made corresponding to the optimum amount of deceleration.

The results of this investigation are shown in figure 15. It is seen that the error in the drag coefficient is equal to or less than 1.1 percent for Reynolds numbers greater than 1×10^4 at all Mach numbers considered. Errors are larger at subsonic Mach numbers and low Reynolds numbers due to the lack of sufficient velocity decrement in the flight trajectory. Accurate measurements at low Reynolds numbers can be made in the APR. This results from the small-size sphere that can be tested in this facility, allowing sufficient deceleration to occur during a flight. A study similar to that just discussed on the number and location of measuring stations was presented in reference 7.

CONCLUSIONS

Ballistics ranges allow extremely accurate drag coefficients of spheres to be measured over a wide variation in Mach numbers and Reynolds numbers. To obtain the maximum accuracy at a specified Reynolds number, care should be exercised in selecting the size of the sphere, the material for sphere fabrication, and the pressure of the test gas. These three parameters should be selected to obtain the optimum amount of deceleration during a flight. Accurate measurements can be made in the transonic region

82

if the velocity decrement is maintained at 10 percent or less.
Spheres should be fabricated from materials with sufficiently
high strength to eliminate the possibility of distortion during
the high-acceleration launch phase of a test.

REFERENCES

1. Krumins, M. V.: Drag and Stability of Various Mars Entry
   Configurations. 19th Congress of the International
   Astronautical Fed, IAF Paper RE 138, Oct. 1968.

2. Hoerner, S. F.: Fluid-Dynamic Drag. Published by author,
   148 Busteed Dr., Midland Park, N. J., 1958.

3. Schlichting, H.: Boundary Layer Theory. McGraw-Hill Book Co.,
   Inc., 1955.

4. Shapiro, A. H.: The Dynamics and Thermodynamics of
   Compressible Fluid Flow.
   Vol. I. Ronald Press Co., c.1953.
   Vol. II. Ronald Press Co., c.1954.

5. Tsien, H. S.: Superaerodynamics, Mechanics of Rarefied
   Gases. Jour. Aeronautical Sci., vol. 13, no. 12, Dec. 1946.

6. Synge, J. L., and Griffith, B. A.: Principles of Mechanics.
   McGraw-Hill Book Co., Inc., c.1942.

7. Karpov, B. G.: The Accuracy of Drag Measurements as a
   Function of Number and Distribution of Timing Stations.
   BRL Rept. No. 658, Feb. 1948.

Figure 1.- NOL 1000-foot Hyperballistics Range.
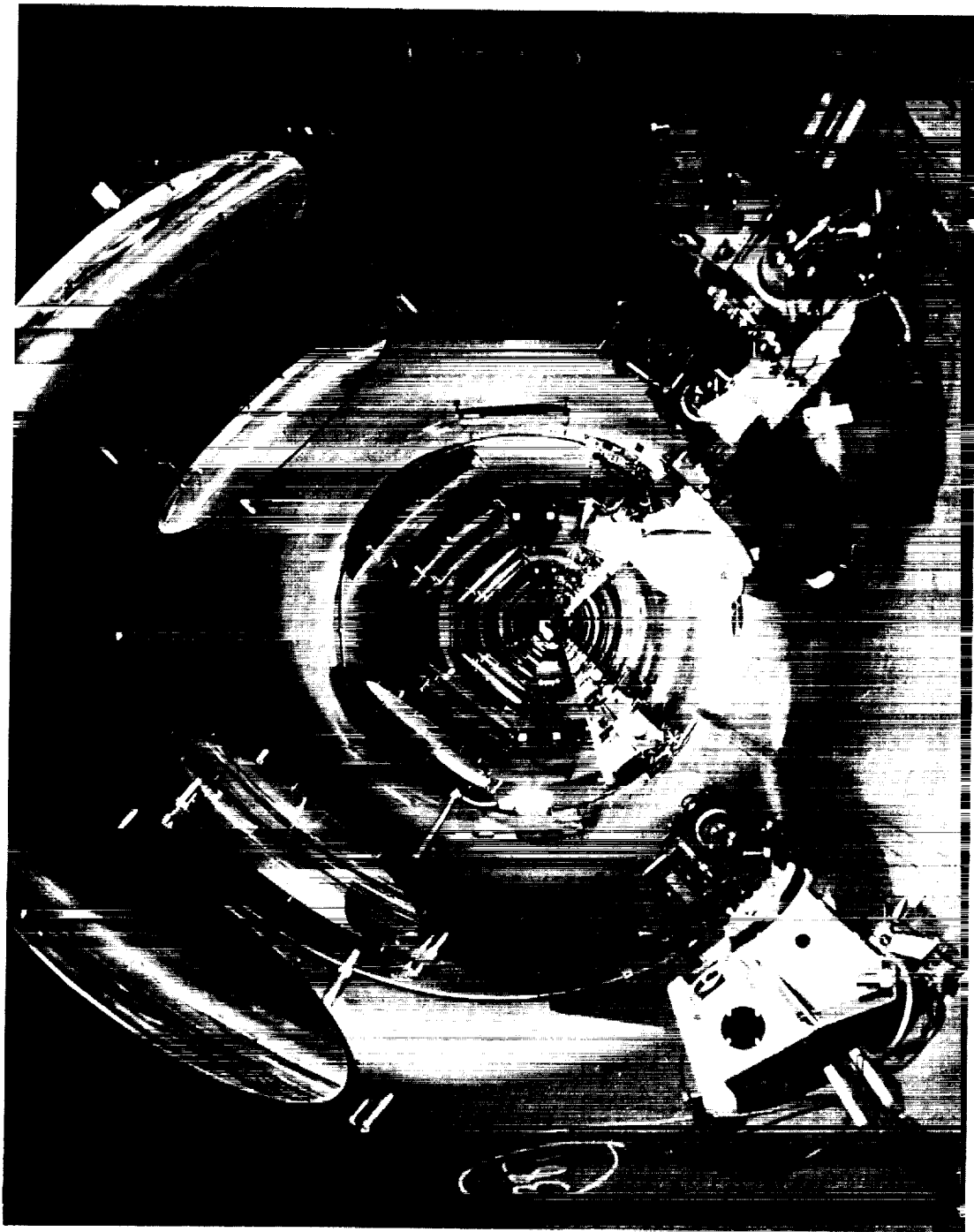
Figure 2.- Inside NOL 1000-foot Hyperballistics Range.

REFLECTOR MOUNT

48-IN.-DIAMETER SPHERICAL REFLECTOR

10-FT-DIA. 1,000-FT RANGE TUBE

USEFUL FLIGHT ZONE

SHADOWGRAPH AND PHOTOGRAPHIC ASSEMBLY

LENS, F/2.5 7" F.L. AERO EXTAR

LIGHT SOURCE

22-IN.-DIAMETER NOMINAL FLIGHT COVERAGE

PHOTO PLATE HOLDER

PHOTO PICK UP

SPARK HOUSING
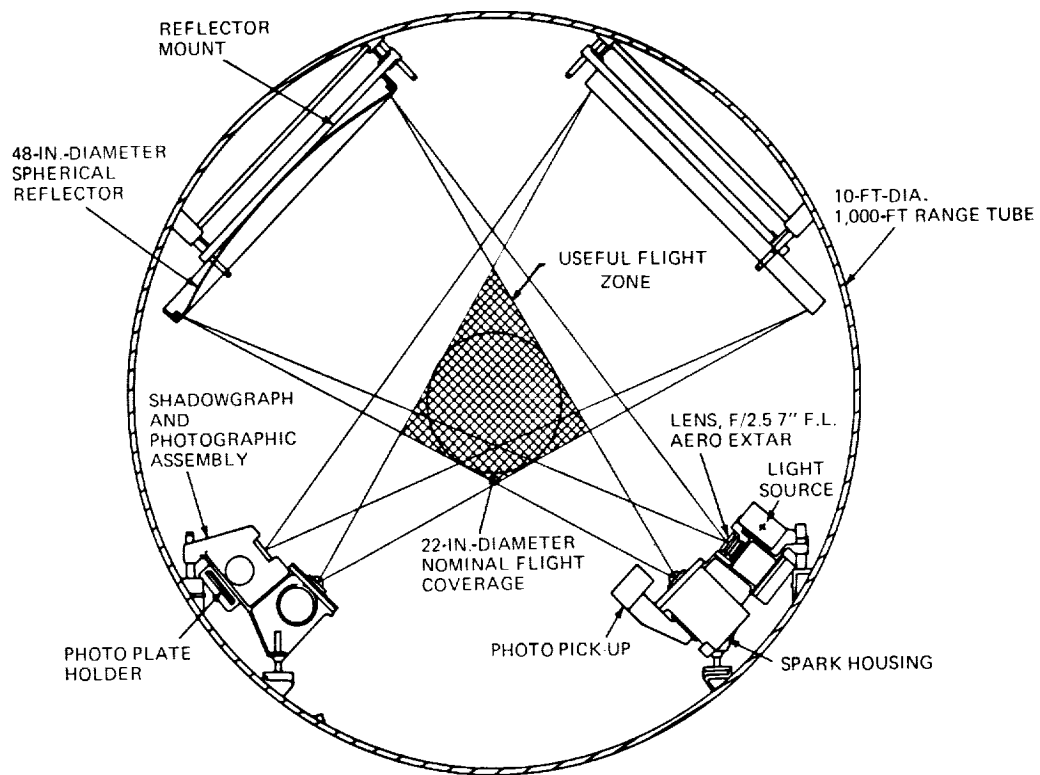
Figure 3.- Schematic drawing of spark shadowgraph station in NOL 1000-foot Hyperballistics Range.
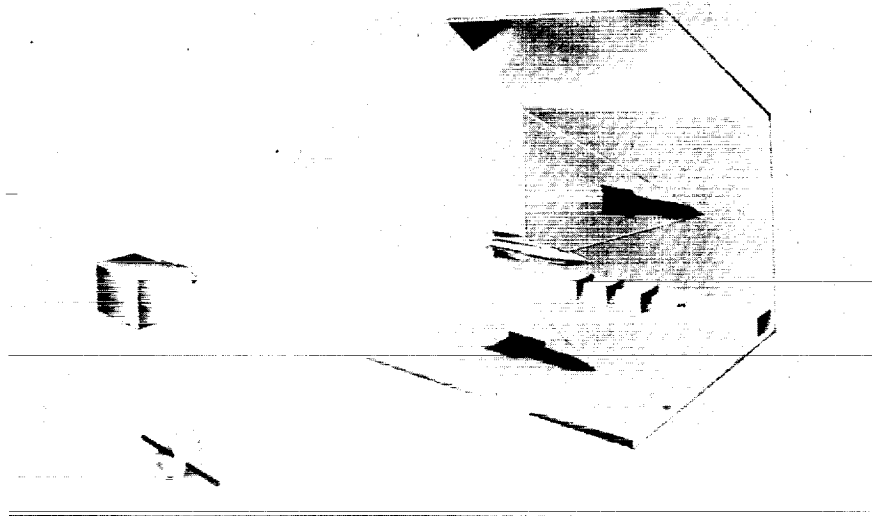
Figure 4.- Schematic drawing of shadowgraph station in NOL Pressurized Ballistics Range.

86

Figure 5.- NOL Aerophysics Range.

32V

87
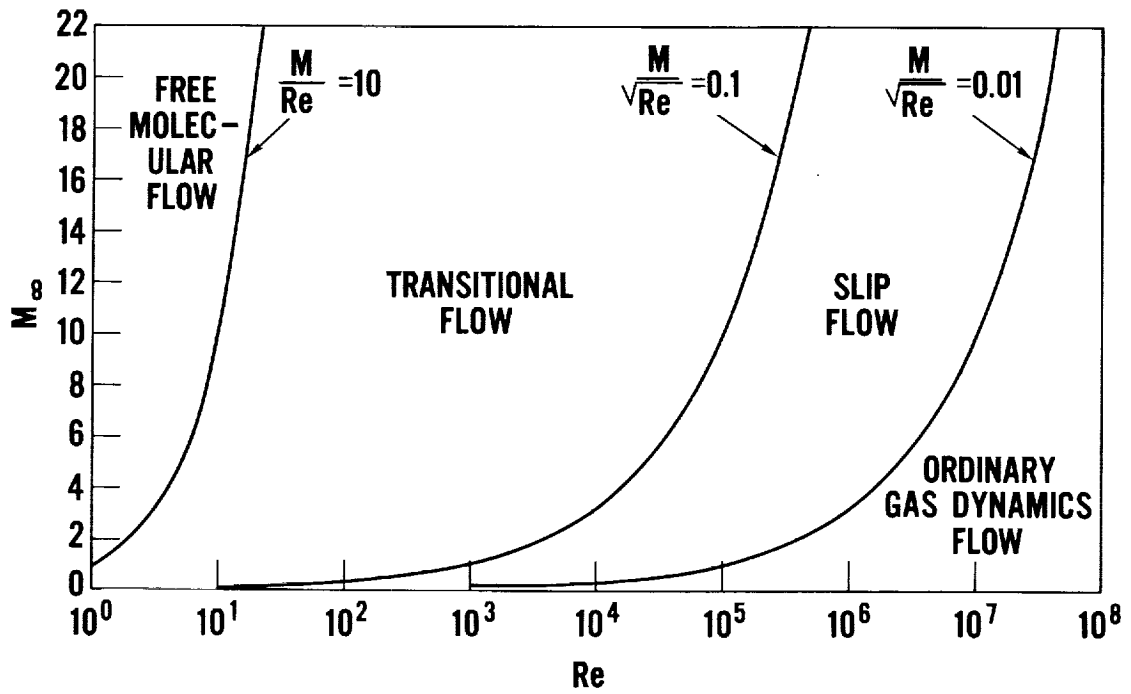
Figure 6.- Flow regimes.
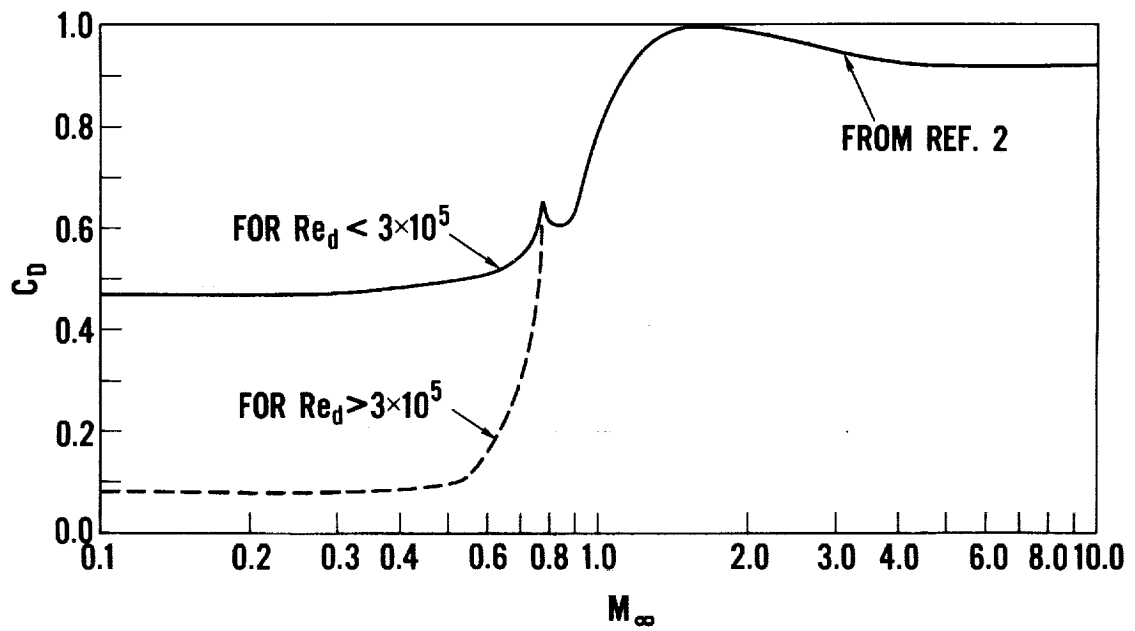
Figure 7.- Drag coefficient for sphere in continuum flow.

88

$$\frac{M}{Re_d} = 10 \qquad \frac{M}{\sqrt{Re_d}} = 0.1$$

DIA. (IN.)	WT. (LBS)
7	11
26.25	0.11
39.37	2.65
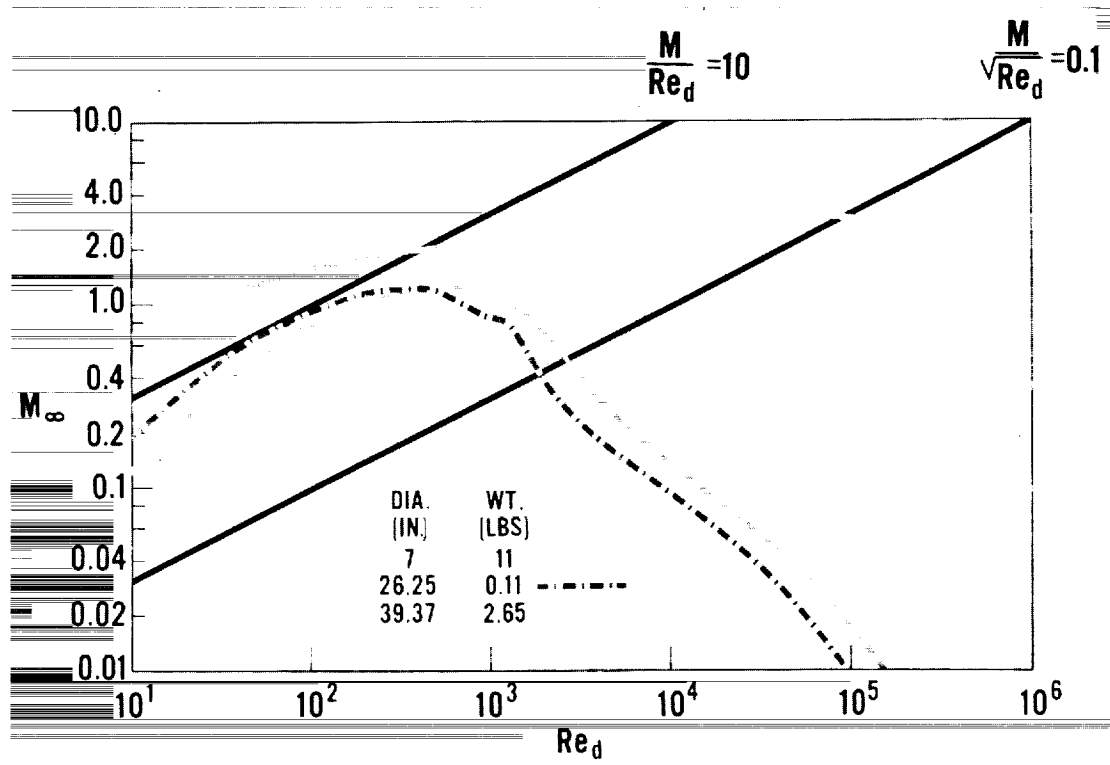
Figure 8.- Trajectory of free-falling spheres.

HYPERBALLISTICS RANGE
2-INCH LIGHT GAS GUN

PRESSURIZED BALLISTICS
RANGE 1.3-INCH LIGHT
GAS GUN
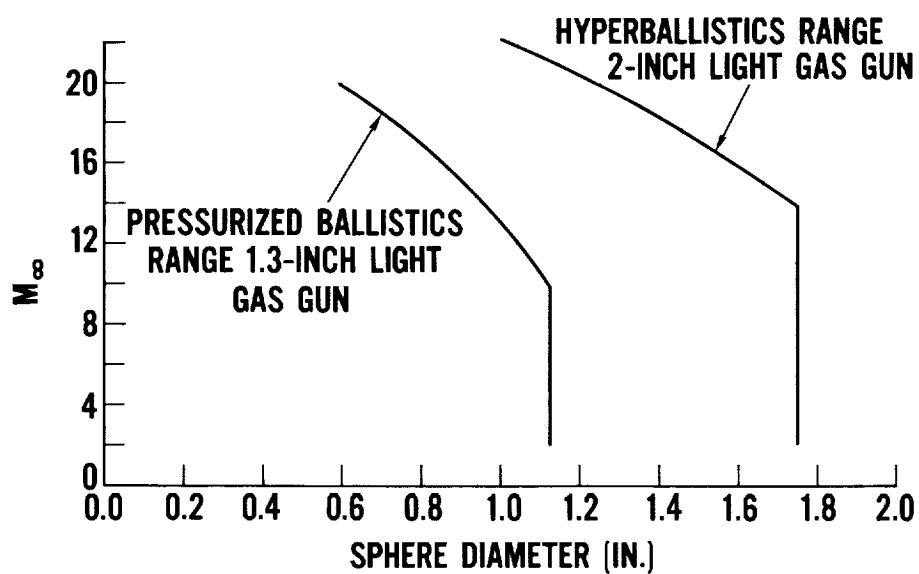
SPHERE DIAMETER (IN.)

Figure 9.- Maximum diameter of spheres that can be launched from light gas guns in
Hyperballistics Range and Pressurized Ballistics Range.

89
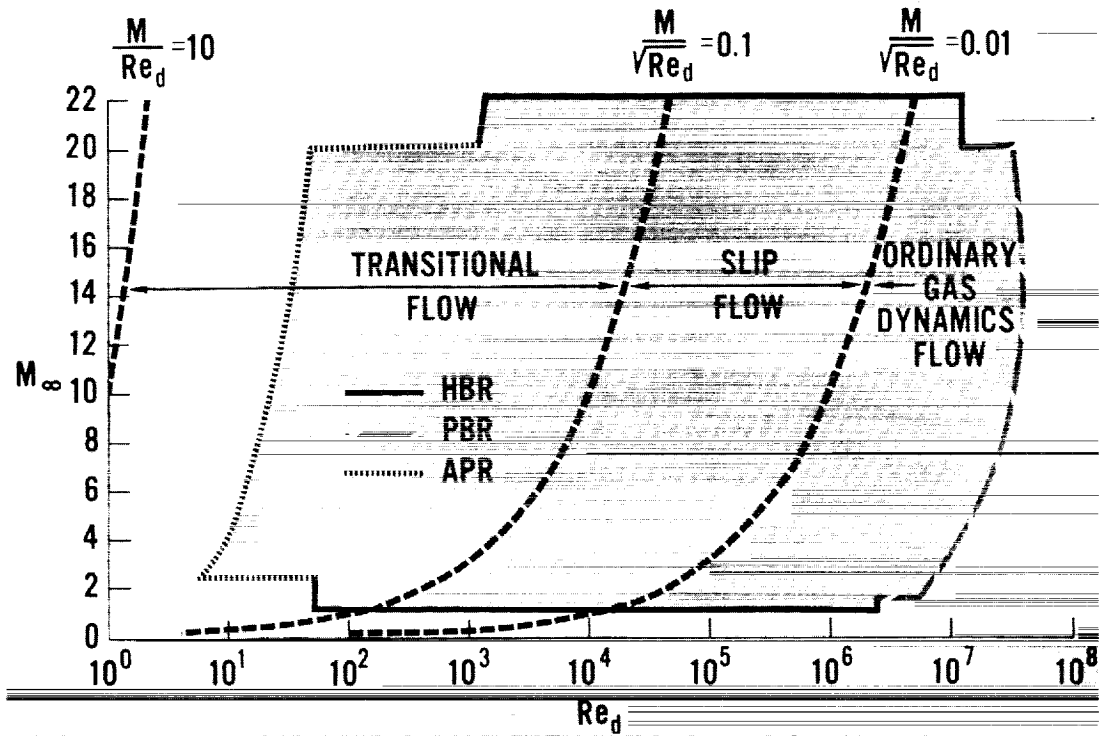
Figure 10.- Mach number-Reynolds number capability of NOL ballistics ranges for spheres in supersonic and hypersonic flight.
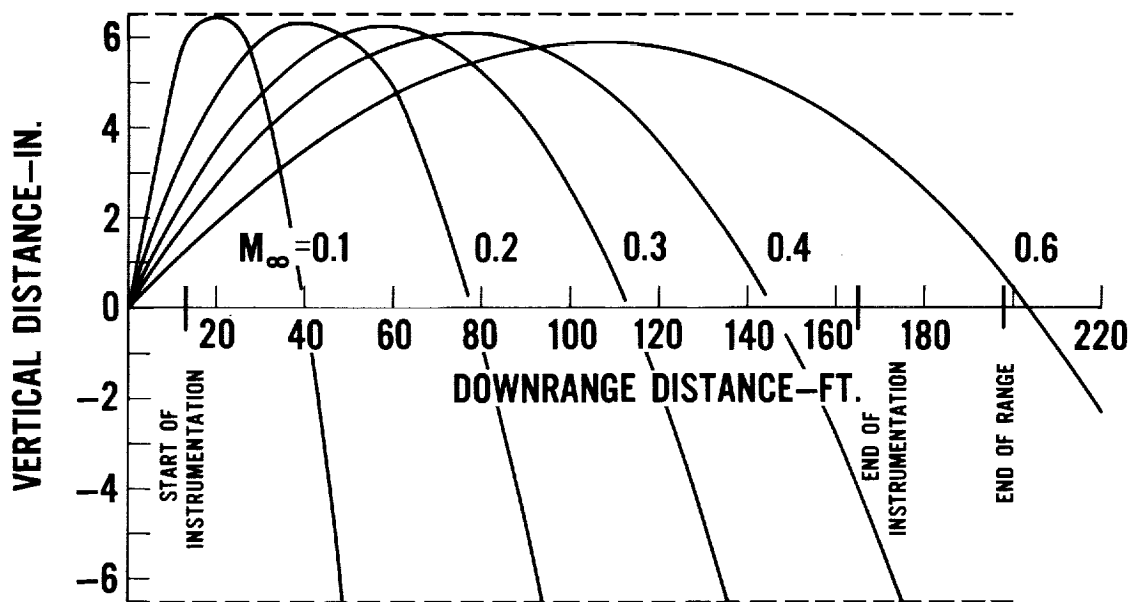
Figure 11.- Sphere trajectories in NOL Pressurized Ballistics Range.
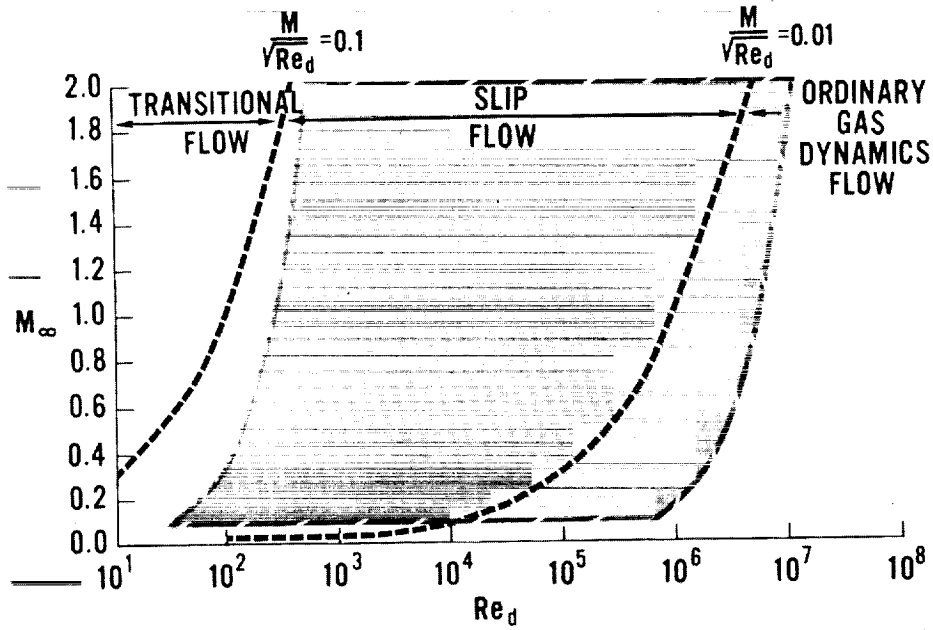
Figure 12.- Mach number-Reynolds number capability of NOL Pressurized Ballistics Range for spheres in subsonic and supersonic flight.
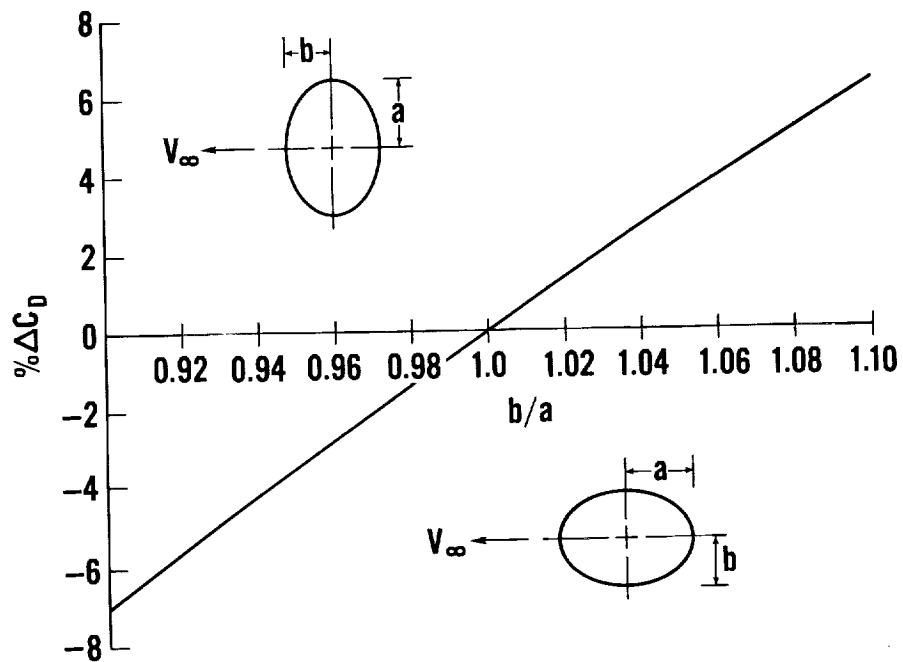

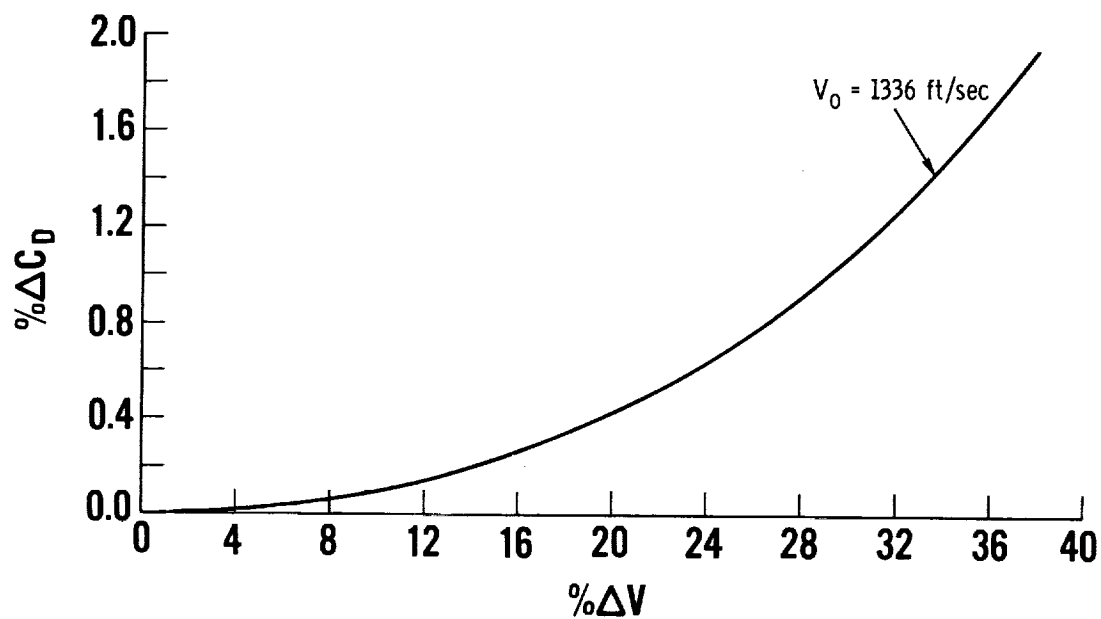Figure 13.- Error in sphere drag coefficient due to distortion.

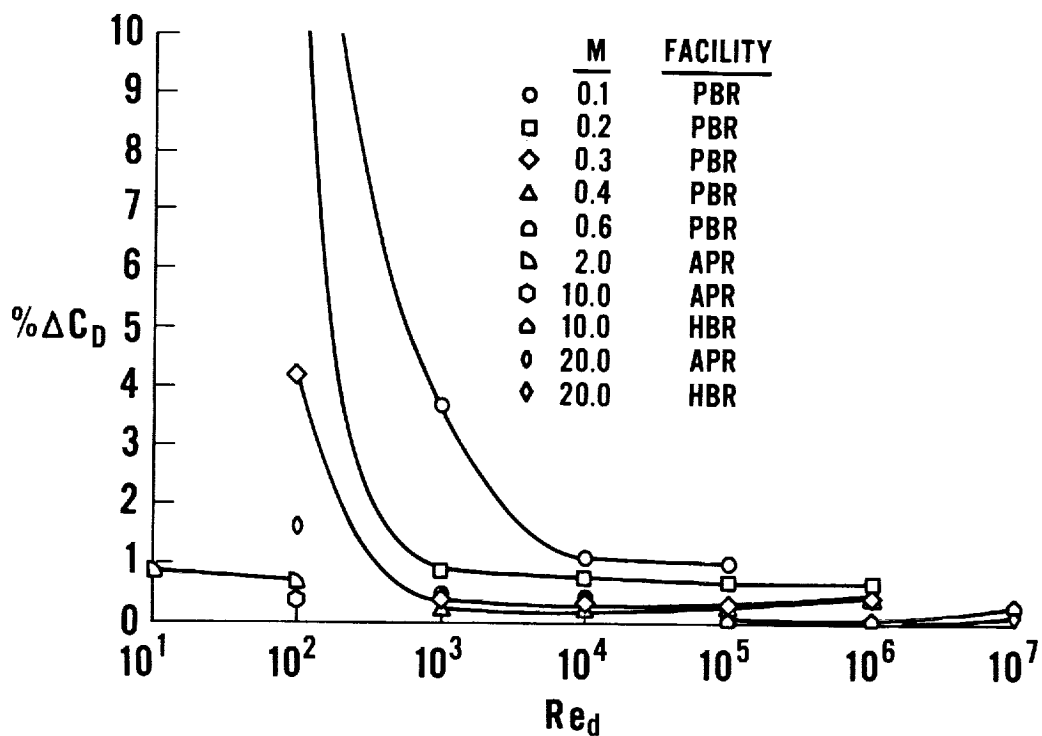Figure 14.- Error in sphere drag coefficient due to constant C_D.

Figure 15.- Error in sphere drag coefficient due to error in distance, number, and distribution of measurements.